crystals

MDPI

Review

Germanium Single Crystals for Photonics

Grigory Kropotov [1], Vladimir Rogalin [2] and Ivan Kaplunov [3,*]

[1] Tydex LLC, St. Petersburg 194292, Russia; grigorykropotov@tydex.ru
[2] IEE RAS, St. Petersburg 191186, Russia; v-rogalin@mail.ru
[3] Tver State University, Applied Physics Department, Tver 170100, Russia
* Correspondence: kaplunov.ia@tversu.ru

Abstract: Germanium (Ge) is a system-forming material of IR photonics for the atmospheric transparency window of 8–14 μm. For optics of the 3–5 μm range, more widespread silicon (Si), which has phonon absorption bands in the long-wave region, is predominantly used. A technology for growing Ge single crystals has been developed, allowing the production of precision optical parts up to 500 mm in diameter. Ge is used primarily for the production of transparent optical parts for thermal imaging devices in the 8–14 μm range. In addition, germanium components are widely used in a large number of optical devices where such properties as mechanical strength, good thermal properties, and climatic resistance are required. A very important area of application of germanium is nonlinear optics, primarily acousto-optics. The influence of doping impurities and temperature on the absorption of IR radiation in germanium is considered in detail. The properties of germanium photodetectors are reported, primarily on the effect of photon drag of holes. Optical properties in the THz range are considered. The features of optical properties for all five stable isotopes of germanium are studied. The isotopic shift of absorption bands in the IR region, caused by phonon phenomena, which was discovered by the authors for the first time, is considered.

Keywords: germanium (Ge); single crystal; IR and THz optics; laser; nonlinear optics; acousto-optics; thermal imager; absorption; scattering; impurity

Citation: Kropotov, G.; Rogalin, V.; Kaplunov, I. Germanium Single Crystals for Photonics. *Crystals* **2024**, *14*, 796. https://doi.org/10.3390/cryst14090796

Academic Editor: Eamor M. Woo

Received: 30 July 2024
Revised: 22 August 2024
Accepted: 28 August 2024
Published: 9 September 2024

1. Introduction

Germanium is the first material based on which solid-state electronics products were manufactured and the development of microelectronics began [1,2]. To do this, it was necessary to develop a technology for purifying raw materials from impurities and growing high-quality single crystals, which led to an active process of a wide variety of studies of its physical and chemical properties. Over several years, thousands of articles and dozens of monographs devoted to this material have been published.

The properties of Ge turned out to be extremely sensitive to the content of even minor concentrations of impurities, especially electroactive ones. Therefore, at the first stage of research, one of the main directions was the technology of obtaining the purest material. Later, it became clear that their structural perfection has a significant impact on the operational properties of single crystals. At the next stage, in connection with practical application, as well as economic factors, it became necessary to obtain single crystals of maximum possible size.

As a result, at present, there already exists an industrial technology for producing dislocation-free germanium single crystals [3]. The content of electroactive impurities has been reduced to a level of 10^{-10} cm^{-3} and even less [3]. The diameter of the grown single crystals of quite decent quality has been brought to the value of 500 mm [4]. Figure 1 shows a photograph of a block of antireflected output windows made of Ge single crystals with a diameter of 420 mm of the experimental 4-beam laser complex [5,6]. Large-sized germanium single crystals for this task were obtained by the method of directional crystallization on a seed crystal. The growth direction was <111>; the grown crystals had the

shape of a disk with a diameter of 420 mm and a thickness of 65 mm. The method was developed and is being implemented at Tver State University. The method is conservative; the main advantage is the absence of crystal stretching; the presence of a limited amount of melt; a uniform temperature field, providing low thermal stresses in the crystal.

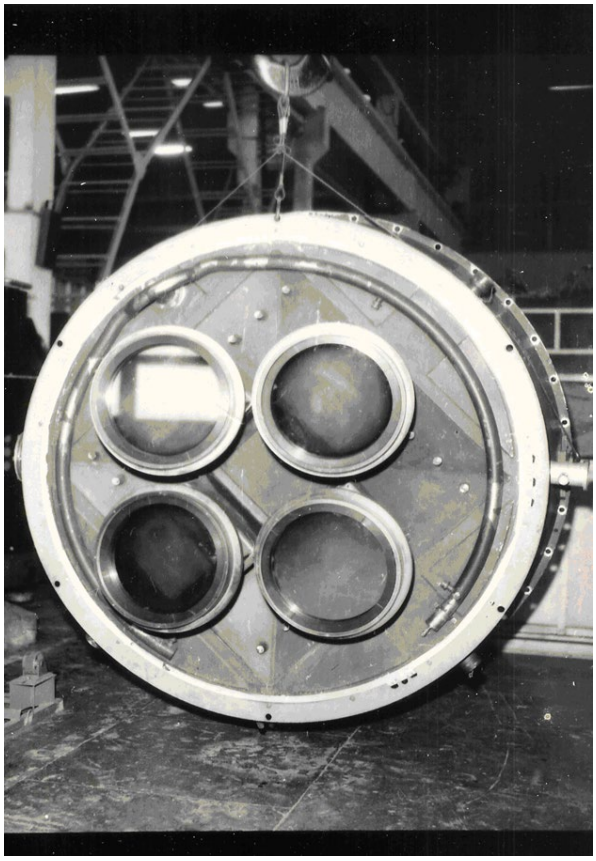

Figure 1. Block of output windows made of Ge single crystals with a diameter of 420 mm of the experimental 4-beam laser complex. Reprinted with permission from Ref. [6]. 2013, Center for Scientific Periodicals NUST MISIS.

Initially, the main consumer of germanium was semiconductor electronics [1,2]. A significant number of different microelectronics components were created on the basis of germanium. Industrial production of dozens of brands of single-crystal germanium has been established, differing from each other in the content of alloying additives, structural perfection, which fundamentally changing the operational properties of the material [3,4,7].

When such industrial production was established, it turned out that n-type germanium is one of the best optical materials for the infrared (IR) region of the spectrum [8]. It is transparent in the range of 1.8–23 μm, and in the range of 2–11 μm, absorption losses were reduced to a level of ~0.015–0.02 cm^{-1} [8–11]. However, in the range of 11–23 μm, a number of phonon absorption bands were discovered, sharply limiting its use in this range; a transparency window was also revealed in the THz range (~100–300 μm) [12].

For two atmospheric transparency windows (ranges 3–5 μm and 8–14 μm), active development of various optical devices began in the post-war years, the most widespread of which were thermal imaging devices [1]. However, the development of IR technology was largely constrained by the shortage of transparent optical materials, in connection with which crystalline germanium (mono- and polycrystals) began to be widely used in these devices.

In the visible region, there is a significant number of different optical materials, mainly based on different brands of glass, and there are proven technologies for their production, processing and operation [13]. In the IR region of 3–5 μm and 8–14 μm ranges, most transparent materials are crystals and have huge operational disadvantages [9]. Among them are water-soluble alkali–halide crystals, soft, plastic crystals of the KRS group (based on toxic thallium salts), etc. It turned out that, based on a set of physical and chemical properties (transparency, hardness, mechanical and climatic resistance, etc.), germanium turned out to be the most preferable material for a number of applications in IR technology, primarily for the optics of thermal imaging devices [1,14]. Later, polycrystalline ZnSe was developed for this region of the spectrum, which in a number of cases has better optical properties (higher transmittance, lower absorption coefficient, transparency in the visible range) [15–17]. Nevertheless, although ZnSe displaced Ge, it could not completely replace it.

The earth's crust contains $7 \cdot 10^{-4}$% by weight of germanium [1,18]. It would seem that this is not a small amount, but in non-ferrous metal deposits, germanium is a much dispersed associated element, and its extraction is very difficult. The main share of Ge is extracted during the processing of zinc ores. In addition, the extraction of germanium from coal is considered economically advantageous when its content is more than 0.5 g per ton of coal. So far, only one deposit (in Belgium) has been explored in the world where germanium-containing minerals are mined. In 2021, the total world production of germanium was estimated at about 140 tons. Therefore, the price of polycrystalline zone-refined germanium usually fluctuates in the range of $1200–1300 per kg [18].

Obviously, for the modern needs of the electronic and optical industry alone, this is extremely little, and the price of the material is quite high. In addition, there are a number of other applications of this material that are not related to photonics and electronics. In the electronic industry, germanium has been almost completely replaced by silicon, which was due to both the cost and the low thermal stability of the semiconductor properties. Currently, more than 200,000 tons/year of monocrystalline silicon are produced in the world at a price of ~$19,000/t [18,19]. Optical silicon is widely used in devices operating in the 3–5 μm range, but in the 8–14 μm region, it is practically not used due to the presence of phonon absorption peaks in this region [19,20]. However, in the terahertz region, silicon has proven to be an extremely popular material.

The use of germanium is currently effective in cases where the use of this expensive and scarce material provides a real, not only technological, but also economic effect. Since germanium does not interact with atmospheric moisture, is non-toxic, durable, has good thermal properties and a high refractive index—n = 4.0 [8], this material remains in demand in IR optics.

The high hardness of Ge (6.0 on the Mohs scale) allows the formation of high-precision optical parts that are well-antireflected even by single-layer ZnS or As2S3 coatings (radiation transmission up to 98%); in addition, a wear-resistant diamond-like antireflective coating can be applied to germanium. Ge is used to manufacture semitransparent mirrors that operate both with and without interference coatings, high-precision Fabry–Perot standards, acousto-optic elements, and other components [1,3,7,21–29]. Narrowband interference filters are usually manufactured on Ge substrates. The most important application area of Ge is the optics of thermal imaging cameras in the wavelength range of 8–14 μm, used in passive thermal imaging systems, infrared guidance systems, night vision devices, fire extinguishing systems, etc. [1,28,30]. Due to its low distortion and high refractive index, Ge is used to manufacture optical elements for spectroscopy that operate on the effect of multiple total internal reflection (MTIR) [2], as well as wide-angle lenses.

At present, for example, in medicine and metal science, various devices using X-ray radiation are widely used. High-quality single crystals with relatively high reflectivity are used as X-ray monochromators. They are oriented in such a way that the surface is parallel to the diffraction planes. The reflected monochromatic radiation obtained in this way is always polarized to a certain degree. The degree of polarization of the radiation depends

on the perfection of the monochromator single crystal. Pure Ge is used for these purposes due to its high refractive index, as well as the achieved high technological level of perfection of the crystal structure [18].

Impurity Ge crystals are actively used to manufacture highly sensitive photodetectors for recording IR radiation [2]. Their operation is based on the excitation by a quantum of radiation of the carrier, located at the impurity level and passing into the conduction band. For different areas of the IR range, a corresponding doping additive is used. As a rule, for the operation of such photodetectors, it is necessary to use forced cooling, usually to the temperature of liquid nitrogen, and in some cases, liquid helium. The range of such photodetectors is quite extensive, and a discussion of their properties is reflected in specialized literature [30–35]. It is important that a structured antireflective surface can be created for germanium-based photodetectors [36].

Nevertheless, we considered it possible to report on the properties of germanium photodetectors for recording radiation from powerful pulsed CO_2 lasers based on the photon hole drag effect [37–40], since their properties turned out to be close to the subject of this publication.

Unlike most traditional optical materials, Ge has specific features that must be taken into account during operation. First, it is highly sensitive to the impurity content in the crystal, which requires a careful approach to selecting the crystal parameters for a specific application. It is also necessary to take into account the lack of transparency in the visible region, the large value of the refractive index n = 4.0, and the presence of an exponential temperature dependence of the absorption coefficient.

Ge single crystals for optical applications are usually grown from a melt using the Czochralski, Stepanov, directional crystallization, and other methods [1,8,18,41]. Sometimes, when absorption and scattering losses in the optical system are insignificant, cheaper polycrystalline Ge is used, which has somewhat higher losses.

For the production of germanium detectors of ionizing radiation, a technology has been developed for growing high-purity single crystals with a concentration of electroactive impurities of less than 10^{10} cm^{-3} [1,3,42–46]. High-purity germanium single crystals (HPGe) are used to create X-ray and gamma radiation detectors, as well as for fundamental research [42,43]. Isotopically pure ^{76}Ge single crystals are planned to be used in the experiment «Large Enriched Germanium by Neutrinoless Double Beta Decay» (LEGEND) to search for neutrinoless double beta decay [44].

At the same time, background electrically neutral impurities, such as oxygen (the concentration of which can reach 10^{17} cm^{-3}), carbon, nitrogen, etc., are always present in germanium. Initially, it was believed that the presence of these impurities does not affect the semiconductor properties of germanium, so little attention was paid to methods of deep purification from these impurities. However, it turned out that the presence of oxygen in germanium single crystals leads to the formation of dislocations, microdefects, and thermal donors, which, in turn, affects the lifetime of nonequilibrium charge carriers and causes losses due to radiation scattering.

The electrophysical and optical parameters of Ge are closely interrelated, which is due to the dependence of the absorption coefficient on the concentration of electroactive impurities, even at relatively low concentrations. Due to this feature, it became possible to successfully test Ge blanks for IR photonics based on measurements of specific electrical resistance (ρ) and conductivity type [8,10,11].

Taking into account that natural germanium is a mixture of its stable isotopes, the optical properties of all five germanium isotopes in the range of 0.2–3000 μm were studied in [47–49]. For isotopes, an isotopic shift of phonon absorption bands in the IR region was recorded, discovered for the first time.

Germanium has a number of nonlinear properties. It should be especially noted that germanium is an acousto-optic material with unique properties, including in the THz range [8,50–56].

Ge is currently used to manufacture transparent optics components for thermal imaging devices; moreover, germanium is a system-forming material for IR photonics for the atmospheric window of 8–14 μm. Ge components are used in a large number of optical devices where mechanical strength, good thermal properties, and climatic resistance are required. The share of various applications is about 25–30% of the total consumption of this material [8].

2. Absorption and Scattering of Germanium in the IR Region of the Spectrum

Many authors [2,23,57] have studied the absorption of IR radiation in Ge; the initial studies were mainly conducted in the field of fundamental absorption or on doped samples. The advent of CO_2 lasers stimulated studies of the absorption coefficient (β) at a wavelength of 10.6 μm. A physically permissible level of the absorption coefficient was revealed and technologically confirmed for practical use. The papers [10,11,58] present the results of a study of infrared radiation absorption in n-type Ge single crystals depending on the specific electrical resistance (ϱ), temperature (T), and wavelength (λ) [59]. Figure 2 shows the frequency dependencies of the absorption coefficient in the region of maximum transparency (2.5–11) μm, the spectral dependence of absorption, and the effect of specific resistance on absorption [5].

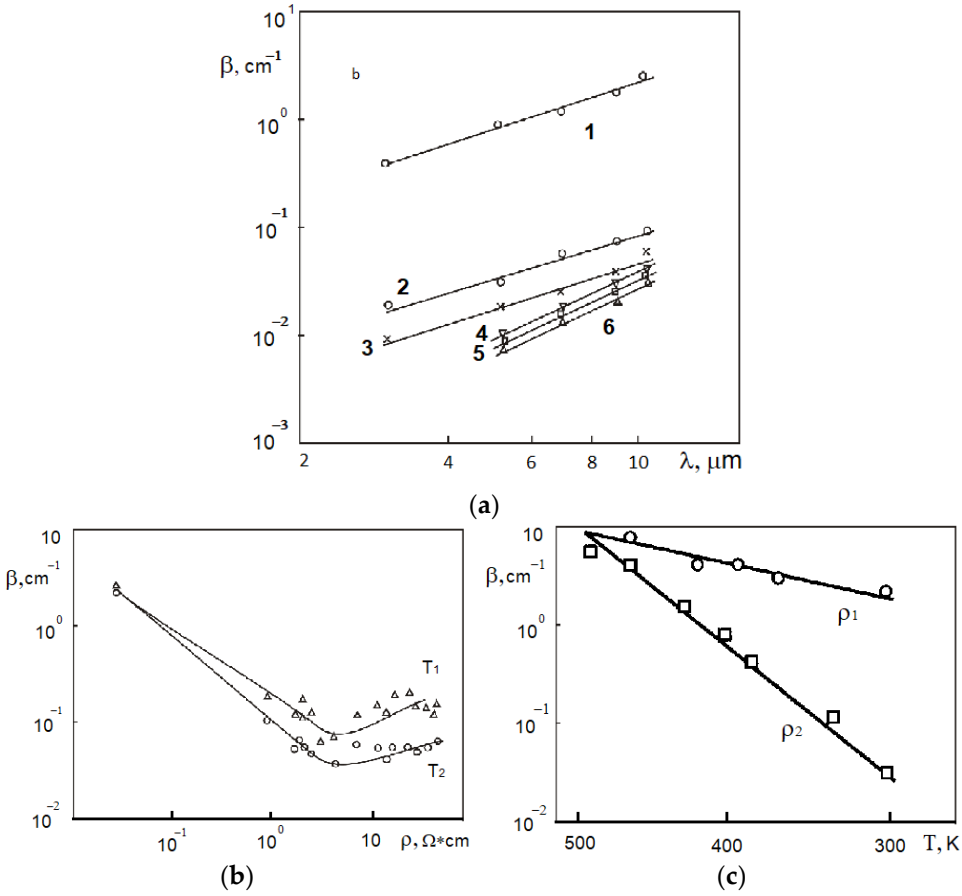

Figure 2. Dependence of the absorption coefficient of n-type germanium in the region of maximum transparency: (**a**) on the wavelength λ (μm): 1. ϱ = 0.03 Ohm·cm; 2. ϱ = 1.0 Ohm·cm; 3. ϱ = 2.0 Ohm·cm; 4. ϱ = 2.5 Ohm·cm; 5. ϱ = 3.0 Ohm·cm; 6. ϱ = 5.5 Ohm·cm; (**b**) at λ = 10.6 μm on the specific resistance, T_1 = 297 K, T_2 = 220 K; (**c**) on the temperature (λ = 10.6 μm): $ϱ_1$ = 0.03 Ohm·cm; $ϱ_2$ = 2.5 Ohm·cm. Reprinted with permission from Ref. [5]. 2015, Rogalin V.E.

In the region of maximum transparency of Ge, optimization of the specific resistance allowed a reduction in the value of β. The measured value of β, strictly speaking, is the value of the attenuation coefficient in the samples (except for the use of the calorimetric

method, which allows for obtaining data only on absorption, but this method allows for measuring the value of β only at the wavelength of the laser used). At present, crystals with $\beta = 0.015$ cm^{-1}, with lattice absorption $\beta_{grat} = 0.01$ cm^{-1} have been obtained. It was possible to bring surface absorption to $\beta_{surf} = 0.0009$ cm^{-1}. These values are close to the technological (phonon) limit of the material's capabilities [10,11,58,59]. The dependence $\beta = f(\lambda)$ obeys the experimental expression $\beta \sim \lambda^{1.2}$ measured by us. The value of β depends exponentially on temperature, and the main mechanism of losses in the volume is absorption on free charge carriers.

Studies of the IR absorption of Ge in the region of maximum transparency have shown that by optimizing the concentration of electroactive impurities, it was possible to reduce the absorption coefficient almost to the phonon limit. This is ensured by the constancy of the ratio of the product of the concentration of electrons and holes and thus reducing the concentration of holes (the absorption cross-section of which, in the 10 μm region, is ~16–100 times greater than that of the electrons [10,11,58,59]). For the production of IR optics from germanium, exclusively crystals of the electron conductivity type are specially grown in the range of specific electrical resistance values of ~5–40 Ohm·cm [22]. It can also be noted that the use of germanium under elevated temperature conditions requires values ~ in the range of 4–10 Ohm·cm. It has been established that doping germanium with silicon increases the temperature stability of transmission, in which a decrease occurs with increasing temperature already at 45–60 °C [22].

However, optical losses can be caused not only by volume absorption but also by surface absorption, as well as by scattering of radiation by structural defects. This can apparently explain some excess of the spectrophotometrically measured value of $\beta_{10.6}$ over the calorimetric measurements [10,11,58,59], where only volume absorption was recorded at $\lambda = 10.6$ μm. These same effects probably led to a decrease in the value of the power coefficient γ in the measured frequency dependence $\beta \sim \lambda^{\gamma}$ [59]. As shown in [2], in the region of small values of β for Ge, the value of the coefficient γ should be ≈2.

With the advent of technology for forming optical parts using high-temperature deformation, an attempt was made to carry out this process when germanium optics are produced. It has been established [60] that plastic deformation leads to a noticeable increase in the absorption coefficient of germanium single crystals. It turned out that changes in the absorption spectrum and conductivity indicate that dislocations arising as a result of deformation at room temperature have acceptor properties.

In the presence of scattering [21,23], the Bouguer–Lambert law for light attenuation is not strictly satisfied, and the known formulas relating transmission and attenuation with noticeable scattering become inaccurate. The differences increase with the growth of the ratio of the probabilities of scattering and absorption of photons in a layer of unit length, and the greater the ratio of the length of the crystal to its diameter, the greater this ratio [26].

For a number of applications, primarily thermal imaging (receiving, processing, and transmitting images), scattering leads to a decrease in image contrast and resolution [15,16]. In this range, small-angle Mie scattering occurs, and the proportion of scattered radiation can reach 20% or more, depending on the characteristics of the specific part made from germanium. Due to the scattering of radiation at the grain boundaries, Ge polycrystals scatter light several times more intensely than single crystals. The scattering coefficients of Ge (10^{-3}–10^{-1} cm^{-1}), corresponding to these losses β_{sc}, are included in the light-weakening (attenuation) coefficients. In many samples, they are comparable with the extinction coefficients themselves and often exceed the value of β [23,25]. Scattering of radiation in Ge occurs due to the presence of growth thermoelastic stresses, impurity inhomogeneity, and structural defects. Maximum scattering is observed in doped mono- and polycrystals with a large number of defects (low-angle boundaries, inclusions, block structure) [21,61]. High-temperature annealing of crystals leads to a decrease in the intensity of light scattering by several times, which indicates a change in the size and shape of the

scattering inhomogeneities, and, possibly, their partial disintegration. During heat treatment of germanium crystals, the following two processes occur: dissociation of oxygen complexes with antimony during heat treatment (with removal of antimony from the impurity cloud) and growth of oxygen clouds due to oxygen diffusion. The use of ultra-pure raw materials, improvement of Ge growth technologies, and high-temperature annealing of grown crystals makes it possible to reduce the loss coefficient [23].

The presence of a sharp temperature dependence of β limits the use of optical elements made of Ge in continuous lasers. Germanium windows in gas lasers operate satisfactorily at radiation power densities of 100–250 W/cm^2 if they can be effectively cooled [9]. However, the use of Ge in continuous lasers has virtually ceased after the creation of optical elements from polycrystalline zinc selenide obtained by the CVD method. Although this material has much worse mechanical properties, it has better optical speed and is much less sensitive to temperature changes.

A connection has been revealed between the crystal structure and electrical conductivity (and, consequently, absorption) of not only single crystals, but also optical polycrystals of Ge, as well as high-purity germanium (HPGe). The electrical conductivity of Ge polycrystals decreases with decreasing grain size, which is associated with a decrease in the mobility of charge carriers caused by their scattering at the crystallite boundaries. The electrical conductivity increases with decreasing crystallites size, and the lifetime of nonequilibrium charge carriers in it decreases due to an increase in the concentration of surface electron states [62].

Dislocation-free and low-dislocation germanium is grown for the production of ionizing radiation detectors, where crystals with a linear defects content (no more than 100 cm^{-2}) and a concentration of electroactive impurities at the level of 10^9 cm^{-3} are required. It turned out that one of the harmful impurities that affects the defect structure and properties of Ge single crystals is oxygen [O] [63–66]. Oxygen in germanium, as a rule, is an atomic optically active interstitial impurity. The complexes formed by [O] in the crystal lattice of germanium are due to the presence of Ge–O–Ge quasimolecules, as well as various GeO_x precipitates, the sizes, concentrations, and shapes of which depend on the total concentration of [O], the growing conditions, and subsequent heat treatment. In works [65,66], the authors established a connection between the oxygen concentration and the dislocation density, determined the content of optically active [O] in Ge crystals of various grades, and found that the presence of oxygen impurity has a noticeable effect on the structural perfection of single crystals and on the parameters of devices manufactured on its basis. The content of optically active [O] in Ge of different grades was determined using FTIR spectroscopy from the position of absorption bands in the phonon region. Regulation of the [O] content in the Ge crystal lattice is often achieved by doping with rare earth elements [67]. It has been shown that when Ge is doped with a number of lanthanides, they actively bind oxygen atoms into electrically neutral complexes, thus formally reducing the concentration of optically active [O] in the matrix by almost an order of magnitude.

Modern technologies for growing germanium single crystals with low oxygen content in crystals should ensure an oxygen concentration at the level of 10^{15} cm^{-3}, which implies growing in an atmosphere with a partial pressure of oxygen in the gas phase not exceeding $1.53 \cdot 10^{-23}$ atm. ($1.5 \cdot 10^{-18}$ Pa). When Ge grows from a melt in the presence of oxygen in the gas phase, a reaction of Ge oxidation occurs with the formation of heterogeneous oxide inclusions GeO_2 in the melt, which are a source that stimulates not only the formation of dislocations, but also the growth of IR radiation scattering on these inclusions [66].

For example, HPGe can be doped with hydrogen during single-crystal growth using the Czochralski method in an H2 atmosphere, which reduces the presence of O-centers. The H_2 concentration in this case is ~10^{-15} cm^{-3}. The presence of a moderate density of dislocations, which are sinks, can facilitate the annihilation of some point defects. For single-crystal HPGe, the minimum density of linear dislocations and the maximum possible value of the concentration of optically active [O] were determined [13].

3. On the Use of Germanium in Space

Interest in Ge has increased in connection with the development of global satellite networks and other telecommunication projects [18]. For on-board power supply of artificial Earth satellites (AES), which form the basis of such projects, radiation-resistant photoelectric converters (PEC) with high efficiency are required. They were developed based on epitaxial structures of AIII–BV GaIn (GaInAs) Ge on substrates of Ge single crystals. Such converters are significantly more expensive than the commonly used silicon ones, but in this case, their use is justified due to a much higher efficiency (more than 39%). The necessary requirements for Ge are a low dislocation density (at a level of no more than 200–250 cm^{-2}) and the absence of dislocation defects, such as low-angle boundaries with a crystal diameter of ≥100 mm [63,64].

Ge-based optics are widely used in space, since this material has high radiation resistance [68]. Ge samples were irradiated with ^{60}Co γ-rays at 3800 rad/s (dose 10^8 rad), fast electrons with an energy of 1 MeV, in a nuclear reactor with a flow of slow and fast (up to 30%) neutrons at T = 200 °C. The IR transmission changed only after processing in the reactor. Thermal neutron irradiation of Ge leads to the formation of Ga and As atoms, which are electroactive impurities and the excess charge carriers thus formed increase the absorption coefficient. When irradiated at 200 °C, a significant proportion of radiation defects (point defects caused by fast neutrons and electrons, as well as gamma rays) are annealed. These are now well-proven results (using electrical methods, optical methods, EPR, etc.) [69–72].

With the development of laser technology, the range of necessary photoelectric converters (PECs) has changed significantly [73]. Such PECs are used for remote power supply of electronic devices and instruments, recharging of unmanned aerial vehicles, and wireless transmission of energy to an autonomous or remote object using laser radiation of different wavelengths λ. There are also medical applications—for recharging implantable prostheses, sensors, and stimulators. The main task in designing and manufacturing such PECs is the conversion of laser radiation into electrical energy with minimal losses.

The possibility of using germanium-based PECs to convert laser radiation with wavelengths of 850, 980, 1310, and 1550 nm is being considered [74,75]. The wavelength of 1550 nm is of significant interest, as it falls into the transparency window of the atmosphere and optical fiber and is relatively safe for vision. This makes it possible to create wireless systems for receiving and transmitting energy in the atmosphere and systems based on fiber-optic communication lines.

The efficiency of conversion of a monochromatic laser radiation (λ = 1550 nm) of germanium-based PECs significantly exceeds the coefficient of efficiency of similar solar cells. The theoretical maximum value of the monochromatic coefficient of efficiency for a given wavelength is ~45% [76]. Unfortunately, the experimental results achieved so far are significantly inferior to the theoretical ones.

The paper [76] examines the possibility of realizing high values of coefficient of efficiency with a relatively simple structure of a germanium-based converter and a reproducible manufacturing technology. Formation of a high-quality p–n junction and reproducibility of the technology were ensured by diffusion doping with zinc from the gas phase. With uniform irradiation of small-sized germanium-based PEC, a monochromatic (λ = 1550 nm) with coefficient of efficiency of 20% was experimentally obtained.

4. Isotopic Shift of Fundamental Absorption Bands of Germanium in the IR Region

The vast majority of data on the physical and chemical properties of Ge were obtained using a material with a natural isotopic composition: Ge (atomic number 32, atomic mass 72.59) consists of a mixture of five stable isotopes with mass numbers 70, 72, 73, 74, 76. The separation of isotopes is a technically complex and expensive process; therefore; there are few data on the influence of isotopic composition on the physicochemical properties of Ge. In work [47], the influence of isotopically purity was studied on the isotopes ^{70}Ge

and ^{74}Ge, and it was shown that isotopically pure germanium at low temperatures has a thermal conductivity 8.5 times higher than natural Ge.

Phonon absorption significantly limits the use of Ge in optics [10,11,59]. The residual absorption of radiation in the IR region and thermal conductivity are largely determined by one physical phenomenon—the behavior of the atoms of the crystal lattice, in other words, phonon processes. They have been well studied; the position of the absorption bands in the spectra of Ge of natural composition is practically a constant of the material. However, on ^{70}Ge and ^{74}Ge samples, an isotopic shift of these bands in the region of 12–14 μm was detected [48] (these measurements were carried out on the same samples as in [47]). This fact was subsequently confirmed for the remaining germanium isotopes, ^{72}Ge, ^{73}Ge, ^{76}Ge [49], and the area of study of absorption bands was expanded to 40 μm, due to which it was possible to significantly expand the number of absorption peaks considered (up to 16).

In this series of experiments, another technology for obtaining pure germanium isotopes was already used, but this did not affect the results obtained (Figure 3). It should be noted that the influence of crystallographic orientation and growth technology on the position of the phonon absorption band maxima was also not revealed. Lattice absorption peaks at frequencies ν—850, 755, 650 cm^{-1}, etc., observed in Ge of natural composition, shifted in monoisotopic crystals, depending on the mass composition of the single crystal. In this case, in ^{70}Ge and ^{72}Ge crystals, an increase in the frequency of the absorption band, ν, is observed, while in ^{73}Ge, ^{74}Ge, ^{76}Ge, ν decreases compared to crystals of natural composition. This shift, although small, exceeds the measurement error and can be used for express assessment of the isotopic composition of Ge.

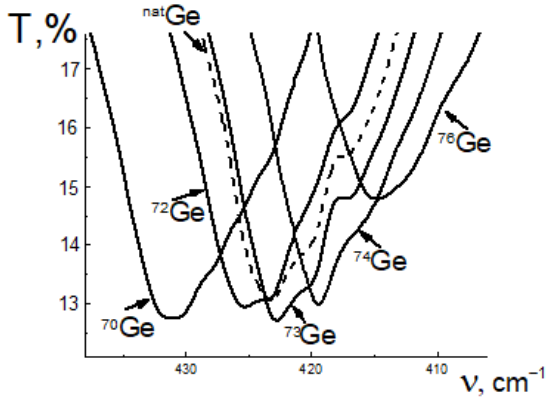

Figure 3. Dependence of spectral transmittance (T), demonstrating the position of absorption peaks in the spectra of samples of natural (^{nat}Ge) and monoisotopic germanium crystals (the mass numbers of isotopes are indicated: ^{70}Ge, ^{72}Ge, ^{73}Ge, ^{74}Ge, ^{76}Ge) in the frequency range of the spectrum 407–438 cm^{-1} (corresponds to λ = 11–40 μm).

Figure 4 shows the dependence of the frequencies ν of the peaks of the phonon absorption of isotopically pure germanium single crystals on the mass number of the isotope, M. In the general case, the shift of the absorption bands was approximated by the following expression (1):

$$\nu = 1.6\nu_0 e^{-k\mathrm{M}}, \quad (1)$$

where ν_0 is the frequency of the maximum of the corresponding phonon absorption band of natural germanium; M is the mass number of the isotope; and k is a power coefficient in the range 0.0062–0.0072. This equation was obtained by processing the experimental data presented in Figure 4.

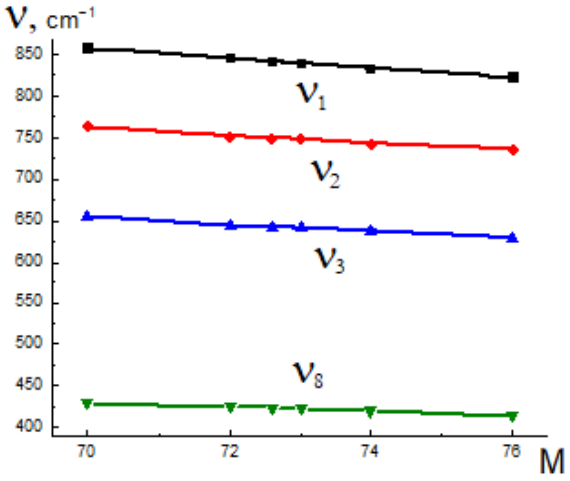

Figure 4. Dependence of the frequencies ν of the peaks of the phonon absorption of the isotopically pure germanium single crystals on the mass number of the isotope, M. Reprinted with permission from Ref. [48]. 2015, Pleiades Publishing, Ltd.

Absorption peaks corresponding to frequencies shown in Figures 3 and 4 [49] can be characterized as corresponding to two-phonon absorption at critical points of the Brillouin zone (active IR modes).

Increasing the operating efficiency of acousto-optical IR modulators based on germanium is largely determined by the increase in the speed and power of devices. The relatively high absorption coefficient of germanium suggests the presence of good heat dissipation during operation of the devices. The efficiency of heat dissipation can be increased by using isotopically pure germanium. Studies of the effect of isotopic purity on the thermal conductivity of germanium have shown that at a temperature of 15 K, the thermal conductivity of the ^{70}Ge isotope is 8.1 times higher than that of germanium of natural isotopic composition, and at a temperature of 20–25 °C, this difference is 20% [77]. In addition, the prospects for the possible use of isotopically pure germanium in such devices can also be determined by the efficiency of acousto-optic interaction in the working elements of the devices. The effect of a reduction in the ultrasound absorption coefficient by more than 2 times at low temperatures [78] in isotopically pure germanium is known, which should be taken into account when assessing the possibilities of using such a material.

The perfection of the crystal structure of germanium can determine the speed of photodetectors operating, for example, on the effect of photon drag of holes. The mobility of minority charge carriers (primarily holes) will depend on the degree of ideality of the crystal lattice, which will be significantly higher for isotopically pure germanium. In particular, this statement for germanium is confirmed by the increase in the thermal conductivity of isotopically pure crystals, caused by the phonon component of the process [78].

5. Optical Damage of Germanium at a Wavelength of 10.6 μm

Ge is a classic semiconductor with a band gap of 0.67 eV [2]. The band gap of germanium is indirect [2], thanks to the various nonlinear effects occurring when intense laser radiation interacts with Ge. The experiments were carried out on a powerful pulsed CO_2 laser setup, shown in Figure 5 (pulse duration up to 5 μs; pulse energy up to 820 J).

Figure 5. Experimental setup for studying the characteristics of pulsed electric discharge CO_2 lasers and the effect of their radiation on materials. Laser cuvettes with Brewster windows made of NaCl single crystals with a diameter of 300 mm. Reprinted with permission from Ref. [5]. 2015, Rogalin E.

The laser parameters are described in detail in [79]. The 3000 mm-long laser resonator was formed by a concave mirror made of oxygen-free copper with a curvature radius of 40,000 mm and a parallel-plane transparent plate made of single-crystal germanium as an output mirror. A single-layer, antireflective coating (arsenic trisulfide—As_2S_3; Fresnel reflection from the germanium surface—R = 0.36) was applied to the outer surface of the output mirror. The capabilities of the laser installation, unlike most studies of optical damage, made it possible to conduct studies by exposing the crystal to a laser beam of a centimeter cross-section. The data obtained differed significantly from the results obtained by focusing the radiation of relatively low-power lasers into a spot with an area of less than 1 mm^2.

Figure 6 shows the typical shape of the laser pulse measured by a photodetector based on the photon drag effect of holes in germanium (1 μs/div). The operation of this photodetector is reported in detail in Section 8 [80].

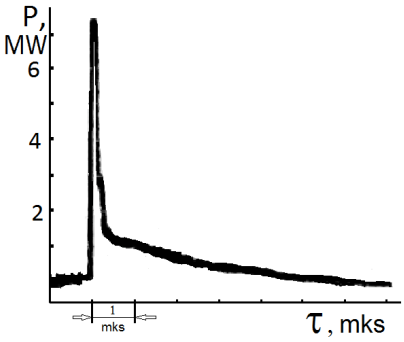

Figure 6. Laser pulse shape measured by a photodetector based on the photon drag effect of holes in germanium.

In the range of power densities of $I = 10^7$–$4 \cdot 10^8$ W/cm^2, the dynamics of propagation of a high-power CO_2 laser pulse through a single-crystal germanium plate was studied [5,6], and nonlinear losses during the passage of the peak part of the laser pulse were determined. At I = 20–50 MW/cm^2, low-threshold optical breakdown of air occurs near the surface of the crystal [5,6,81].

The effect of the leading edge of the laser pulse leads to the appearance of nonequilibrium charge carriers in the surface layer of the crystal, which absorb radiation. In [5,6], nonlinear radiation losses were studied on a group of base crystals, transparent in the region of 10 μm and used for the manufacture of transparent optics of CO_2 lasers. The

radiation losses on them grow exponentially with the decreasing width of the forbidden zone of the crystal. The experimental dependence is described by Formula (2):

$$I_2 = \frac{(1-R)I_1}{\exp(1-\Delta E_g/2kT)}, \quad (2)$$

where T~2.5·10^4 K; ΔE_g is the band gap; R is the reflection coefficient; k is the Boltzmann constant; I_1 is the peak power density of the laser pulse; and I_2 is the power density of the laser pulse transmitted through the crystal.

The intensity of radiation passing through Ge decreases only twofold after 5–10 pulses, and damage is localized exclusively in the near-surface layer. This indicates that Ge is capable of withstanding significant radiation overloads without catastrophic destruction, and the material is of considerable interest for the optics of powerful-pulsed CO_2 lasers [82]. The morphology of damage to Ge after exposure to radiation from a powerful-pulsed CO_2 laser was studied using methods of light and electron microscopy, as well as X-ray tomography [5]. The studies were conducted on serially produced Ge of optical quality treated using a specially developed chemical–mechanical technology modified for use in optics, and on dislocation-free crystals polished using a chemical–mechanical technology used in microelectronics [83]. It was established that in the range of amplitude values of the radiation power density of 2·10^6–4·10^8 W/cm^2, two main types of damage are realized. At a power density of I < 4·10^7 W/cm^2, centers of local microdamages on the surface layer were observed. These local microdamages are the result of microexplosions that form craters on the sample surface [82]. They occur at I < 4·10^7 W/cm^2 due to optical breakdown either on absorbing microinhomogeneities of the crystal or on defects in optical processing. Exposure to radiation at $I \geq$ 4·10^7 W/cm^2 leads to melting of a practically continuous surface layer in the irradiated zone, with a depth of 1–3 μm. This is explained by the avalanche breakdown of nonequilibrium charge carriers of the surface layer of Ge (Figure 7). The molten layer is like a nonlinear absorbing filter, protecting the volume of the optical element from damage by radiation of superthreshold intensity. The nature of the impact, which leads to the destruction of only the surface layer of the optical part, allows for the complete restoration of expensive germanium products through significantly less expensive repolishing.

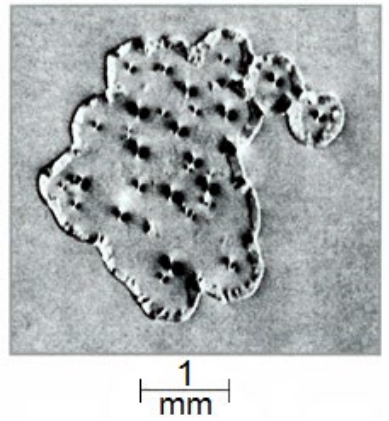

Figure 7. X-ray topogram of the surface of a germanium single crystal after exposure to a CO_2 laser pulse. Peak power density at 20 MW/cm^2 (internal stress fields around emerging structural defects are clearly visible). Reprinted with permission from Ref. [5]. 2015, Rogalin V.E.

Thus, it was shown that the output semi-transparent mirror made of germanium for high-power pulsed CO_2 lasers is practically "indestructible" even in the case of a significant excess of the optical damage threshold. This is an important result, since powerful gas lasers often use a simple semi-confocal resonator, in which the mirrors additionally serve as sealed ends of the laser cell. When pumping the spent working mixture, due to the pressure difference of 1 atm., their surface is subjected to significant mechanical load.

In case of a hidden defect in the output mirror (window), it may not withstand. This leads to catastrophic destruction of the germanium window (mirror), which instantly disintegrates into a large number of fragments. Atmospheric pressure catapults them inside the cuvette, at the same time the fragments fly apart and hit the "blind" metal mirror, causing catastrophic damage and simultaneously disabling the cuvette's electrode system.

6. Nonlinear Absorption of Germanium in the Range of 3–5 μm

When using optical elements made of germanium in laser technology operating in the atmospheric window of 3–5 μm, it should be taken into account that in the range of 2.6–5 μm, in addition to the usual absorption, additional effects of two-photon and three-photon absorption are observed [84,85]. In this case, the process of radiation absorption is nonlinear, and this fact must be taken into account.

In work [86], nonlinear absorption of radiation from a high-power non-chain pulsed HF(DF) laser was investigated on Ge samples of different thickness and specific resistance. Depending on the composition of the active mixture (SF_6:C_2H_6 or SF_6:C_6D_{12}), laser radiation was generated in the range of either 2.7–3 μm (HF laser) or 3.7–4.1 μm (DF laser). The HF laser generation spectrum was a set of 18 different lines in the range λ = 2.6–3 μm (average ν = 0.4397 eV, which corresponds to λ = 2.82 μm). The laser pulse duration at half-height was ~150 ns; the maximum pulse energy was E ≈ 5 J; the energy distribution was close to uniform.

Even at low HF laser irradiation intensities (I = 0.3 MW/cm²) in the absence of visually visible damage to the samples, a significantly nonlinear nature of the passage of radiation through Ge is observed. Figure 8 shows the experimental dependences of the transmission of Ge with a thickness of h = 1 mm on the radiation power density of HF and DF lasers, respectively, and Figure 9 shows the dependence of the concentration of nonequilibrium free-charge carriers generated in the process of two-photon absorption by depth (the calculation was carried out for the time t ~ 200 ns). Nonlinear absorption of DF laser radiation in a germanium single crystal was observed at a significantly higher radiation intensity I > 10 MW/cm². The transmission of Ge in the nonlinearity region decreases significantly with increasing sample thickness and value of crystal resistivity. The power of the transmitted pulse is noticeably reduced; the pulse shape is strongly deformed, and at the same time, a noticeable shortening of the leading edge is observed. The coefficient of two-photon absorption of single-crystal germanium K_2 = 55 ± 10 cm/GW was calculated.

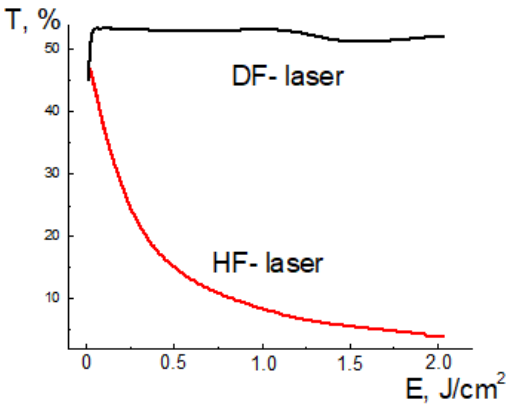

Figure 8. Transmission coefficient of Ge (ϱ = 20 Ohm·cm) with thickness h = 1 mm depending on the incident energy density of HF and DF lasers.

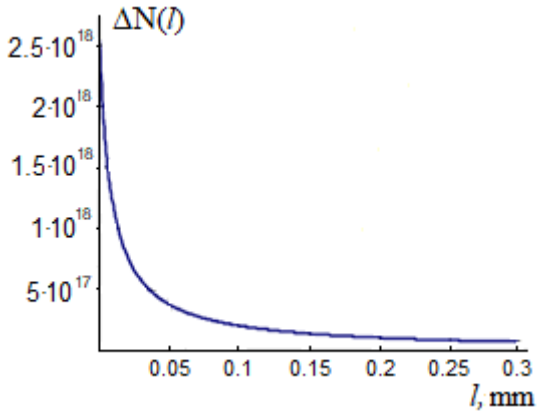

Figure 9. Dependence of the concentration of nonequilibrium free carriers generated in the process of two-photon absorption on the depth (calculated at the time: t~200 ns).

The influence of pulse parameters on the dynamics of the passage of an intense HF laser pulse through Ge samples of different thicknesses (h = 0.03–0.55 cm) is analyzed. The intensity distribution $I(l)$ over the thickness of Ge changes noticeably during the duration of the laser pulse. The generated nonequilibrium carriers are concentrated in a thin layer near the input surface of the crystal (see Figure 8), i.e., the main processes of nonlinear absorption occur in the surface layer less than 50 μm thick. A kind of nonlinear filter arises, as in the case observed when exposed to a CO_2 laser. It prevents the destruction of the material volume even when trying hard to focus the laser energy into the sample volume. This circumstance indicates a large influence of nonlinear absorption of intense laser radiation occurring in the surface layer of germanium. In this case, the value of the recombination coefficient of free carriers on the surface can exceed the volume value by several orders of magnitude. Therefore, special doping of the surface layer makes it possible noticeably change the value of nonlinear transmission of the entire Ge sample.

7. Other Nonlinear Effects in Germanium

When exposed to intense laser radiation, other nonlinear effects are also observed in Ge [2]. The optical constants of the materials are determined by the well-known equation:

$$P = \varepsilon_0(\chi(1)E + \chi(2)E + \chi(3)E + \ldots), \quad (3)$$

where P is the electric polarization induced by the electromagnetic wave; E is the field strength; χ is the susceptibility tensor of the medium.

In linear optics, only the first term of this equation is taken into account, but when working with powerful laser radiation, it is no longer possible to neglect nonlinear effects determined by other terms of the equation. For materials with a diamond structural type (in particular, for Ge), the coefficient $\chi(2) = 0$. However, the next coefficient $\chi(3) = 1.5 \cdot 10^{-10}$ CGSE units (for germanium). Therefore, it was possible to use Ge single crystals for efficient wave front reversal [87]. In a parallel-plane plate made of Ge, installed inside the resonator of a CO_2 laser, phase-conjugate reflection was recorded at λ = 10.6 μm from phase gratings arising in counter-propagating waves. The magnitude of the reflection coefficient reached 20%. The laser beam reflected by such a mirror returns along the same optical path. The use of wave front reversal allows one to obtain diffraction divergence of high-power laser radiation, despite the presence of inhomogeneities in the active medium, in optical elements and in the atmosphere.

One of the possible applications of germanium single crystals in photonics at present is its use for stabilizing the emission frequency of IR laser diodes by generating optical frequency combs (OFCs) based on compact optical microresonators. Optical frequency combs are a set of narrow equidistant spectral lines; generation is possible using both complex setups based on mode-locked femtosecond lasers [88] and on spherical or disk

optical microresonators with «whispering gallery» modes (WGM resonators) [89]. Such WGM resonators have small dimensions and a high-quality factor. The created optical frequency combs have a free dispersion region from units to hundreds of gigahertz and a fixed distance between the lines due to phase synchronization. Microresonators are used to stabilize laser radiation and generate photon pairs for quantum cryptography and communications. Based on microresonators, we can create devices and instruments operating in various fields of science and technology: spectroscopy, communications, telecommunications, navigation, and metrology (creation of reference sources of optical and radio frequencies), etc. [90,91]. The OFC generation effect occurs in optically nonlinear materials when pumped by a continuous laser. In this case, due to the Kerr effect, so-called four-wave mixing occurs, because of which the photons are redistributed between the modes, and an OFC is generated.

Microresonators (1.35 and 1.5 mm-thick) were fabricated based on high-purity germanium (HPGe) [92]. Experimental setups were assembled, which provided excitation of «whispering gallery» modes in microresonators at a wavelength of 2.68 μm using various coupling elements, such as rectangular prisms and hemispheres. A record quality factor was measured, which is $(2.2 \pm 0.3) \cdot 10^7$ and is determined by radiation losses in germanium. It was found that high-quality modes in germanium microresonators provide impulse tightening of a laser diode with a tightening range width up to 100 MHz. The high-quality factor of germanium microresonators indicates the possible use of such devices for stabilizing the frequency of lasers in the IR region of the spectrum.

8. The Effect of Photonic Drag of Current Carriers in Germanium

When studying the time characteristics of powerful-pulsed CO_2 lasers, the active medium of which consists of a mixture of gasses (CO_2; N_2; He), an interesting problem was unexpectedly discovered. The fact is that such lasers in the free generation mode emit powerful pulses with an energy in the range of 1–1000 J, and sometimes more. The pulse duration in this case is several microseconds, and their shape is very specific (Figure 6) [79,80]. The pulse is characterized by an initial peak with a duration of 100–200 ns, the amplitude of which is determined by the concentration of CO_2, and a "tail", the time duration of which depends on the concentration of nitrogen and helium in the working mixture. When working with such a laser, it is necessary to change the composition of the gradually degrading mixture quite often. It turned out that the pulse shape can be noticeably distorted; so, when conducting experiments, it is necessary to register it as accurately as possible. In addition, there are various methods for converting the pulse duration of CO_2 lasers, allowing this value to be changed in a wide range (10^{-3}–10^{-12} s) [93], which also stimulates the improvement of the process of measuring the shape of the laser pulse. When conducting laser experiments, a portion of the radiation is usually isolated for measurements using an optical wedge, which usually reflects ~4% of the radiation. When using a highly sensitive photodetector for measurements, it is often necessary to additionally weaken the radiation entering it many times in order not to go beyond the dynamic range, which reduces the reliability of the measurements.

Initially, photoresistors based on germanium alloyed with impurities of gold, mercury, zinc, etc., or based on CdHgTe compounds were used to measure the duration and shape of CO_2 laser pulses. Their use for these purposes is complicated by the fact that they only allow obtaining high-quality results, since these photodetectors, originally intended for recording weak signals, have excessively high sensitivity for this case, on the order of 3 V/W. When working with powerful lasers (10^6–10^{10} W and more), the radiation must be weakened many times, which naturally does not allow one to count on an accurate quantitative result. In addition, the dynamic range of such photodetectors usually does not exceed 2–3 orders of magnitude. This is clearly not enough for the pulse shape shown in Figure 6. In addition, they typically operate at liquid nitrogen temperature, and in some cases, even lower. Finally, they have a small area of reception platform (usually ~2 × 2 mm^2) and an opaque input window made of a clear germanium plate, which significantly

complicates alignment. The photodetectors described below, based on the effect of photon drag of current carriers, are free from these disadvantages.

The effect of photon drag of current carriers is one of the manifestations of nonlinear phenomena in semiconductors. It was theoretically predicted in [37] and was initially discovered in p-type germanium single crystals under the influence of a pulse of radiation from a powerful CO_2 laser [38,39]. Subsequently, this effect was also discovered in some other crystals when excited by powerful lasers of other frequencies. This effect is of considerable practical interest, since it turned out to be interesting for recording powerful laser pulse radiation [5,40]. In particular, photodetectors for recording powerful pulse radiation of CO_2 lasers were made from p-type germanium single crystals.

The IR radiation incident on the photodetector is absorbed, and in this case, the electromagnetic wave pulse can be transmitted to the charge carriers in the semiconductor, causing the appearance of a directed flow of charge carriers and thereby forming a current of entrainment [38,39]. Emerging EMF is proportional to the power of the incident radiation.

Germanium is a direct-gap semiconductor, in which the maximum energy of the valence band is located at the center of the Brillouin zone, where two valence bands merge, and below is a third valence band, split off from the first two due to spin-orbit interaction [72]. The upper zone corresponds to heavy holes, the next zone to light ones. In this case, the ratio of the masses of heavy holes to light ones is ~8. There are no holes in the third, lower, zone.

Photodetectors based on p-type germanium use direct intraband transitions since the CO_2 laser radiation quantum $h\nu$ = 0.117 eV is absorbed in the crystal mainly due to the intraband transition between the sub-bands of holes with heavy and light masses. The resulting photoEMF is used to register the radiation parameters with λ = 10.6 μm. The sensitivity range is limited from below by equipment noise, and from above by the bleaching effect associated with the impossibility of transitions due to the presence of filled states and due to the competition of hole transition rates caused by the action of radiation and interhole collisions.

In this case, the hole perceives not only the energy, but also the momentum of the photon. The movement of holes relative to the crystal lattice in the direction of radiation propagation occurs due to the need to fulfill the laws of conservation of energy and momentum. In this case, a potential difference arises between the ends of the crystal rod—the photon drag EMF (V). The main advantages of such a photodetector are as follows: time resolution up to 10^{-10} s, large dynamic range (10–10^7 W/cm^2), operation at room temperature, and sensitivity of the order of 0.1–1.0 V/MW. The time constant (τ) of the device is described by a simple Formula (4):

$$\tau = nc/L, \quad (4)$$

where L is the length of the working crystal of the photodetector; n is the refractive index; c is the speed of light.

The laws of conservation of energy and momentum force holes to move in the crystal lattice in the direction of radiation propagation. This initiates the appearance of a potential difference between the ends of the crystal rod—the photon drag EMF (V) (5):

$$V = \frac{CW_{pl}\rho(1-R)}{S\hbar w}, \quad (5)$$

where $C = e(-\tau_h v_h + \tau_L v_L)$ is the constant of the crystalline sample, in which v_h and v_L are the group velocities of heavy and light holes, respectively, τ_h and τ_L are the relaxation times of pulses in two-hole systems, e is the electron charge; W_{pl} is the peak power of the laser pulse; ρ is the specific electrical resistance of the material; S is the area of the receiving zone; R is the reflection coefficient from the input plane of the receiver (for Ge R = 0.36); $\hbar = h/2\pi$ is Planck's constant; ω is the angular frequency of laser radiation.

To obtain the maximum signal, it is necessary to optimize the sample by the following parameters: ϱ, S, L. The maximum value of the measured EMF is observed at the greatest crystal length. However, it is impossible to significantly increase the length due to noticeable absorption of radiation in p-type Ge. In addition, the time resolution decreases. Therefore, when it is necessary to measure subnanosecond pulses, it is necessary to reduce the sensitivity by decreasing the time constant due to shortening the crystal. When measuring the radiation of lasers with relatively "long" pulses, it is more advantageous to use a photodetector with the maximum possible length of the crystal rod.

The paper [40] reports a technical solution that made it possible to combine measurements of subnanosecond and comparatively "long" pulses using a single device. A 6 cm-long p-type Ge crystal rod was manufactured, onto which 7 ohmic contacts were applied at equal distances from each other along the normal to the optical axis of the crystal rod. The device allows recording photo-EMF using any pair of contacts, thereby quickly changing the working length of the crystal rod. Thus, the possibility of operational adjustment of the measured parameter values is achieved. Experimental testing of this photodetector was carried out using a pulsed CO_2 laser [5,79], with output energy of up to 820 J per pulse and a duration of 5 μs.

The maximum measured value of EMF is ensured by optimizing the crystal by the parameters: ϱ, S, L. At room temperature, the optimal values are ϱ ≈ 1–10 Ohm·cm and L = 4–6 cm, and the area of the receiving area corresponds to the minimum possible size of the cross-section of the laser beam [38–40] (Figure 10). It is desirable to take into account that the beam of the laser under study must enter the crystal so that the axis of the crystal coincides with the optical axis. Otherwise, due to multiple reflections from the side faces in the crystal, distortions of the measurement results are possible.

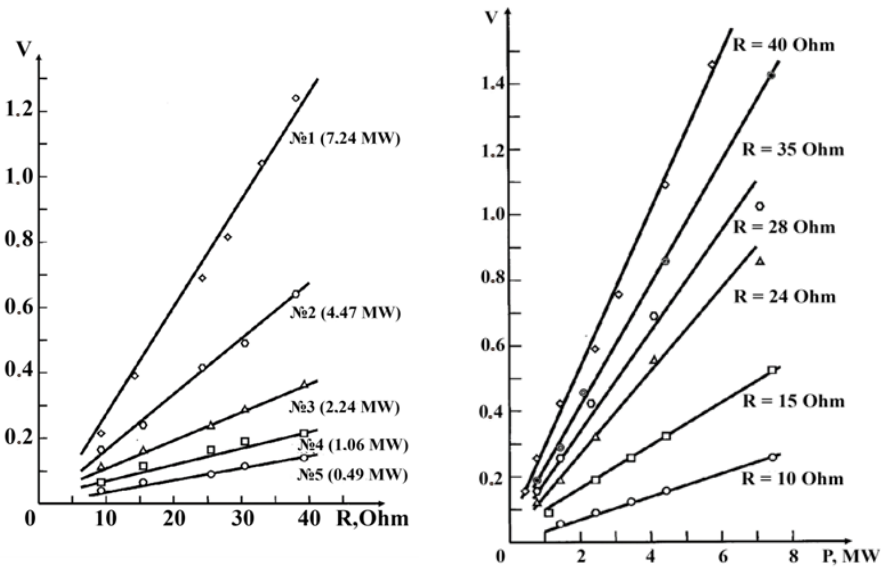

(**a**) (**b**)

Figure 10. Figure 10. Characteristics of a photodetector based on the photon drag effect of holes in germanium: (**a**) volt-watt characteristic of the photodetector; (**b**) dependence of the output signal of the photodetector on the resistance. Reprinted with permission from Ref. [5]. 2015, Rogalin V.E.

Like all nonlinear effects in materials, this effect manifests itself under the influence of intense radiation. In practice, the process is observed at radiation power densities of ~10^5–10^7 W/cm^2. This fact made it possible to create an effective device for measuring the radiation power and energy of powerful-pulsed CO_2 lasers based on a p-type germanium single crystal.

9. Acousto-Optic Effects in Germanium

At present, optical radiation control devices, the operation of which is based on the acousto-optic effect (the interaction of light with sound in an optically transparent medium), are an important component of such a technological section as optical electronics.

The acousto-optic effect (AO) [94,95] is a nonlinear effect; the effect allows one to control all parameters of optical radiation: intensity, frequency, direction of propagation, polarization, frequency, and spatial spectrum. The passage of an acoustic wave in a photoelastic medium induces changes in the instantaneous value of the refractive index, which leads to the formation of a phase grating with a period equal to the length of the acoustic wave and an amplitude proportional to the amplitude of the acoustic wave and the photoelastic constant of the crystal. Such capabilities, combined with purely technological advantages—reliability, compactness, and, as a rule, fairly low power consumption of AO devices, determine the wide application of AO devices.

The modern trend in the development of acousto-optics is associated with the increasing introduction of AO devices into technology, which leads to a constant increase in the production volumes of AO devices in our country and in the world.

In laser technology, acousto-optic devices are used as laser shutters; AO modulators are indispensable for modulating the amplitude and changing the frequency of optical radiation.

AO deflectors are used both to control the direction of propagation of optical radiation (for example, in lidars) and for tunable cylindrical lenses of scanning systems in ultrahigh-resolution optical microscopes.

AO devices turned out to be useful in systems for generating short and ultrashort laser pulses of high and ultrahigh power. Widely used applications of AO devices (Q-switches) include their use for synchronization of longitudinal laser modes.

AO filters are indispensable devices for managing and analyzing the spectral composition of optical radiation, creating compact spectrometers, including imaging ones.

Until recently, the existence of powerful sources of optical radiation in the infrared spectral range was actually limited to the CO_2 laser. At present, quantum cascade lasers have appeared that operate in the spectral range of generated radiation from 2.5 to 300 μm. For example, quantum cascade lasers are used to detect various gasses by absorption lines located in the range from 2.5 to 15 μm. Free-electron lasers, capable of emitting in a wide range of wavelengths, are also being actively developed. They have made it possible to significantly expand the areas of practical use of infrared and terahertz radiation [96]. The sharp increase in the number of practical applications has exacerbated the existing problem of controlling the parameters of optical radiation with such wavelengths. As in the case of shorter wavelengths of optical radiation, the use of AO devices in the thermal IR range seems quite promising. However, the development of AO devices that effectively function in this spectral region is limited by the presence of suitable materials for creating AO cells.

Germanium is one of the main materials in acousto-optics of the mid- and far-infrared ranges, due to its good physical and chemical properties and high values of the refractive index and photoelastic constants [50]; moreover, for CO_2 lasers, it is, today, the only acousto-optic material used. Acousto-optic modulators based on germanium for CO_2 lasers are mass-produced by many companies (see, for example, [51]). Sometimes, Ge is used in the 5–6 μm range, as well as in the 2–3 μm range, where the dominant material paratellurite (TeO_2) has absorption bands [97].

The high thermal conductivity of Ge allows the creation of thermally stable designs of various acousto-optic devices based on Ge single crystals, consuming tens of watts of control power with a diffraction efficiency at a wavelength of 10.6 μm of more than 90% [52]. Water-cooling is usually used to thermally stabilize the working crystal in these devices. In modern technology, laser acousto-optic modulators based on Ge are used for pulse control of laser radiation [53].

The disadvantage of germanium is that the material does not have high AO quality, and to achieve high efficiency of AO interaction, it requires the application of extremely high acoustic power, reaching 200 W. In addition, this requires the use of large, by acousto-optic standards, crystals with water-cooling. In addition, germanium is optically isotropic, and it is difficult to create good AO deflectors and filters on its basis.

10. Plasma Antennas Formed by Laser Radiation in Germanium

As we have already noted, germanium is the most studied semiconductor material. Therefore, studies of some relatively new phenomena are usually initially conducted on germanium samples. After identifying the main physical processes and obtaining the first positive results, the search for more effective or cheaper semiconductors usually begins. Very often, it quickly becomes clear that this search has been successful, and further research is carried out using another, more suitable material. This was repeated in the study of plasma antennas. Further research was carried out on more accessible materials [98].

An interesting direction of modern laser technology is the creation of Ge-based devices for modulating IR and microwave radiation: modulation using controlled introduction of moderate amounts of nonequilibrium excess carriers into the surface layer of a germanium plate by excitation with diode laser radiation [54]; modulation in Ge waveguide structures on silicon substrates by controlling the absorption of free carriers [55,56]. This idea was further developed in the creation of plasma antennas for various radio and telecommunication devices. The work in [99] reports on experimental studies of the efficiency of transmission of high-frequency signals by a semiconductor vibrator-transmitting antenna based on Ge and Si single crystals, on the surface of which, due to the internal photoelectric effect, a nonequilibrium electron–hole plasma is formed by radiation from a laser diode. It turned out that this is a very convenient tool for controlling the electromagnetic properties of objects due to the insignificant energy costs for the formation of nonequilibrium free-charge carriers with a high concentration of charge carriers (10^{16} cm^{-3} and higher). In these experiments, a nonequilibrium electron–hole plasma was created using continuous radiation from a laser diode with a fiber output (λ = 975 nm). The nonequilibrium plasma stimulates the growth of the transfer characteristics of a semiconductor antenna (Figure 11).

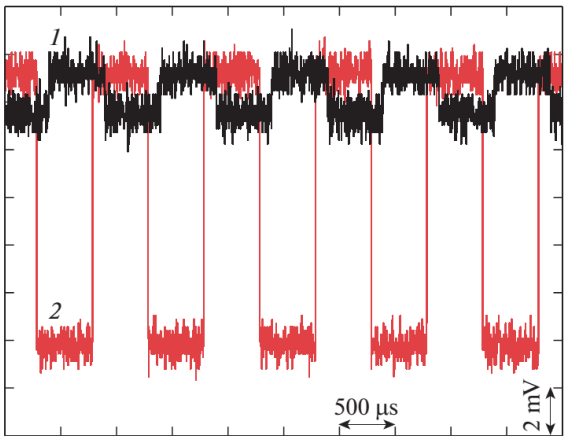

Figure 11. Time series of microwave signals measured at the detector receiver with the laser switched off (1) and laser irradiation (2) of the surface of a single-crystal germanium plate with an incident radiation power of the laser diode P_{las} = 2.64 W. Vertical scale: 2 mV/div; time scale: 500 μs/div. Reprinted with permission from Ref. [99]. 2019, Pleiades Publishing, Ltd.

Figure 11 shows a typical oscillogram of signals on the receiving microwave detector, from an antenna made of a Ge single crystal (a rectangular plate measuring 5 × 45 mm and 1 mm thick, ϱ = 47 Ohm·cm). It is clearly seen that the nonequilibrium electron–hole plasma created by laser action has proven itself as a vibrator plasma antenna.

11. Study of Laser Etching of Semiconductors Using Germanium as an Example

Chemical etching with aggressive acids and alkalis is commonly used in the electronics industry to reveal the structure of a material [100]. Today, this is the standard method for studying the structure of semiconductors. It is known that the dislocation density on germanium is revealed by chemical etching of the {111} plane.

In the process of studying the preparation of material samples for subsequent diffusion welding, in works [101,102], an alternative, environmentally friendly, safe method of promptly identifying the structure of semiconductors by means of the effect of intense frequency-pulse laser radiation on the material was proposed. Single-crystal germanium was used as a model material.

In work [101], studies were carried out on both dislocation-based, industrial germanium, GMO brand, n-type (specific electrical resistance ~ 5 Ohm·cm, doped with antimony at a concentration of ~$3 \cdot 10^{14}$ cm^{-3}), and dislocation-free samples, similar in impurity composition.

The samples were cut from one single crystal, respectively. Samples of the main crystallographic faces were studied. After polishing using conventional optical technology [103], the deviation of the sample surface from the orientation of the planes {111}, {110}, and {100} was less than 10 arc min. The initial surface roughness (before exposure to laser radiation) was 0.5–0.6 nm.

The samples were exposed to scanning-focused pulse-periodic intense radiation of a nanosecond laser (wavelength 355 nm, duration ~10 ns, energy density ~0.5–1.3 J/cm^2, pulse repetition frequency 100 Hz). At a fixed energy density, an area of ~1 × 4 mm^2 was processed. After changing the energy density, another area was processed. About 30 laser pulses fell on the same area of the surface during such processing.

Before and after such treatment, the samples were examined using a Zygo NewView 7300 optical profilometer and a JEOL JSM 6610LV scanning electron microscope (SEM).

Figure 12 shows the {111} surface of dislocation Ge after exposure to scanning nanosecond radiation of a UV laser with an energy density of E = 1.14 J/cm^2 [101]. Traces of "dry" etching, which arose as a result of the radiation, are clearly visible. They are similar to dislocation pits obtained by traditional chemical etching. A similar picture was not observed on other planes of the dislocation crystal, as well as on all three planes of the dislocation-free crystal.

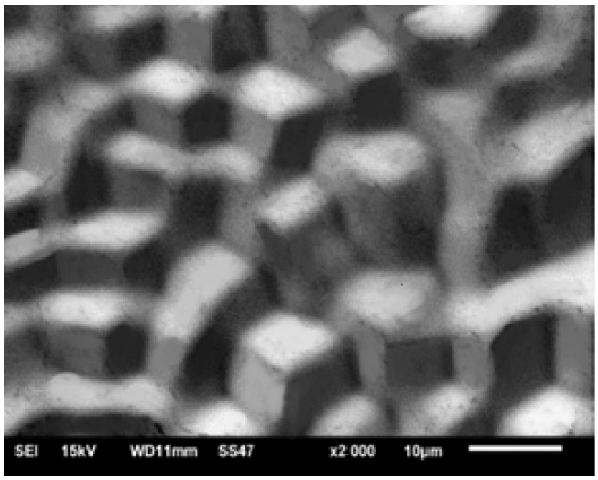

Figure 12. SEM images of the {111} surface of dislocation Ge after exposure to scanning nanosecond radiation of a UV laser with an energy density of E = 1.14 J/cm^2: magnification—×1000. Reprinted with permission from Ref. [101]. 2023, Pleiades Publishing, Ltd.

12. Transmission of Germanium in the THz Spectral Region

Due to the extreme shortage of optical materials, especially nonlinear crystals, for the terahertz (THz) range of the electromagnetic spectrum (~3 mm–30 μm, 3 cm^{-1}–300 cm^{-1})

[104], the possibilities of using germanium in this spectral region have recently been considered. It turned out that the active elements of germanium acousto-optic devices are very interesting for use in this range [105]. In [12], the optical properties of pure and doped Ge in the THz range were studied. It is shown that germanium can be used in multispectral infrared imaging devices of the IR + THz range, as well as for the production of output windows of THz gas lasers with optical pumping by CO_2 laser radiation.

The transmission spectra of Ge with different resistivity ϱ are shown in Figure 13 [12]. The results showed a noticeable increase in absorption in the doped Ge crystals in the THz range compared to undoped (ϱ = 47 Ohm·cm). An increase in the concentration of doping impurities, both electron and hole, leads to an increase in absorption. If in the range of 25–50 μm, the effect of ϱ on the transmission of Ge(Sb) is not noticeable, then in the range of ≥220 μm, it is observed directly.

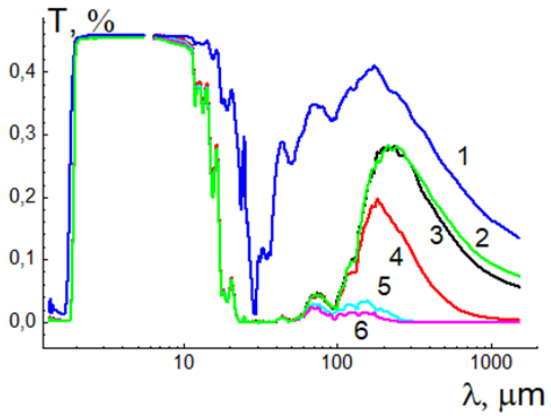

Figure 13. Optical transmission of a Ge single crystal doped with antimony. 1—undoped Ge (thickness 1 mm); 2—undoped Ge; ϱ: 3—46 Ohm·cm; 4—20 Ohm·cm; 5—5 Ohm·cm; 6—2.7 Ohm·cm (spectra 2–6 were obtained on samples h = 10 mm). Reprinted with permission from Ref. [12]. 2019, Pleiades Publishing, Ltd.

The main contribution to the absorption of radiation in germanium single crystals in the THz range is made by free-charge carriers (intrinsic and impurity). If we compare the transmission spectra data for Ge (spectral region λ~160–220 μm) and for silicon [12], they show that the attenuation coefficient in the region of 160–220 μm is approximately the same and is ~0.5 cm^{-1}.

In contrast to the IR range, in the THz region, minimal losses of ~0.5 cm^{-1} are observed in undoped germanium crystals in the region of λ ~160–220 μm. Significant losses due to Fresnel reflection can be largely compensated by creating periodic relief structures on the surface of the optical element with a high degree of regularity and a period shorter than the radiation wavelength. Therefore, optical products made of undoped single-crystal germanium can be used quite effectively to control radiation in the THz range (100–300 μm range).

In [106], the transmission spectra of all five single crystals of isotopically pure germanium were investigated in the THz spectral region. It was shown that the absorption minimum in the wavelength range of 30–3000 μm is observed in the range of 200–800 μm, and the corresponding absorption coefficient for this range is less than 1 cm^{-1} for most of the investigated single crystals of isotopes. In the range of 1000–3000 μm, a tendency was found for the absorption coefficient to increase with increasing mass number of the isotope.

13. Conclusions

It should be noted that germanium (along with silicon) is one of the most studied materials. Therefore, it is often used as a model material in the initial study of little-studied

phenomena. Often, after receiving the first positive results, such studies are continued using more accessible materials.

This study presents the results of many years of research into the optical properties of single-crystal germanium and the applications of this material in IR optics and photonics, carried out mainly by the authors. Germanium is transparent in the spectral range of 1.8–23 μm (although, there are a number of phonon absorption bands in the range of 11–23 μm); a transparency window has been discovered in the terahertz (THz) spectral range (~100–300 μm). Two atmospheric transparency windows in the IR ranges of 3–5 μm and 8–14 μm practically cover the region of maximum transmission of germanium. Crystalline germanium, due to its physical and chemical properties, is one of the system-forming materials of IR optics, and its use in this area is up to 25–30% of the total consumption structure of this material. The use of crystals in optics is significantly affected by impurities, the specifics of obtaining single crystals, and the presence of structural defects. Information is presented on the effect of isotopic purity on the transmission spectra of all five isotopically pure germanium single crystals.

Author Contributions: Conceptualization, G.K. and V.R.; methodology, V.R. and I.K.; formal analysis, V.R. and I.K.; resources, G.K.; writing—original draft preparation, V.R.; writing—review and editing, G.K., V.R., and I.K.; supervision, G.K.; project administration, I.K.; funding acquisition, V.R. All authors have read and agreed to the published version of the manuscript.

Funding: The work was carried out with the financial support of the Russian Science Foundation RSF grant No. 24-19-00727, https://rscf.ru/project/24-19-00727/using the capabilities of the Shared Use Center of Tver State University.

Data Availability Statement: No new data were created or analyzed in this study. The original contributions presented in the study are included in the article; further inquiries can be directed to the corresponding author.

Acknowledgments: The authors express their gratitude to Rogalina A.I. for assistance in computer design of the drawings.

Conflicts of Interest: The authors declare no conflicts of interest.

References

1. Claeys, L.; Simoen, E. *Germanium—Based Technologies: From Materials to Devices*; Elsevier: Berlin, 2007; 449p.
2. Pankove, J. *Optical Processes in Semiconductors*; Prentice-Hall, Inc.: Englewood Cliffs, NJ, USA, 1971; 456p.
3. Umicore. Available online: https://www.umicore.com/en/investors/annual-report (accessed on 10 January 2024).
4. Kaplunov, I.A.; Kolesnikov, A.I.; Gavalyan, M.Y.; Belotserkovskiy, A.V. Optical properties of large germanium monocrystals. *Opt. Spectrosc*. **2016**, *120*, 654–659. https://doi.org/10.1134/S0030400X16030139.
5. Rogalin, V.E. Resistance of Power Optics Materials to the Effects of Powerful Radiation Pulses from CO_2 Lasers. Ph.D. thesis. Tver State University. 2015, 351p. (In Russian)
6. Rogalin, V.E. Transparent materials for high-power pulsed CO2-laser. *Izvestiya Vysshikh Uchebnykh Zavedenii. Materialy Elektronnoi Tekhniki = Mater. Electron. Eng*. **2013**, *2*, 11–18. https://doi.org/10.17073/1609-3577-2013-2-11-18 (In Russian)
7. Germanium and Applications. Available online: http://www.geapplic.ru/en/ (accessed on 10 January 2024).
8. Kaplunov, I.A.; Rogalin, V.E. Optical properties and application of germanium in photonics. *Photonics* **2019**, *13*, 88–106. https://doi.org/10.22184/FRos.2019.13.1.88.106.
9. Bendow, B. Optical properties of infrared transmitting materials. *J. Electron. Mater*. **1974**, *3*, 101–135. https://doi.org/10.1007/BF02654548.
10. Bishop, P.J.; Gibson, A.F. Absorption coefficient of Ge at 10.6 μm. *Appl. Opt*. **1973**, *12*, 2549–2550. https://doi.org/10.1364/AO.12.002549.
11. Capron, E.D.; Brill, O.L. Absorption coefficient as a function of resistance for optical germanium at 10.6 μm. *Appl. Opt*. **1973**, *12*, 569–572. https://doi.org/10.1364/AO.12.000569.
12. Kaplunov, I.A.; Kolesnikov, A.I.; Kropotov, G.I.; Rogalin, V.E. Optical Properties of Single-Crystal Germanium in the THz Range. *Opt. Spectrosc*. **2019**, *126*, 191–194. https://doi.org/10.1134/S0030400X19030093.
13. Brinkmann, M.; Hayden, J.; Letz, M.; Reichel, S.; Click, C.; Mannstadt, W.; Schreder, B.; Wolff, S.; Ritter, S.; Davis, M.; et al. Optical Materials and Their Properties. In *Springer Handbook of Lasers and Optics*; Träger, F., Ed.; Springer Handbooks; Springer: New York, NY, USA, 2007. https://doi.org/10.1007/978-0-387-30420-5_5.
14. Infiniti. Available online: https://www.infinitioptics.com (accessed on 10 January 2024).

15. Marsh, K.J.; Savage, J.A. Infrared Optical Materials for 8-13 μm—Current Developments and Future Prospects. *Infrared Phys.* **1974**, *14*, 85–97. https://doi.org/10.1016/0020-0891(74)90011-6.
16. Fraser, H.; Hope, A.J.N.; Worrall, A.J. Optical Materials and Material Processing for Used with Infra-Red Equipment. In *International Conference Low Light and Thermal Imaging Sistem*; IEEE: London, UK, 1975; pp. 21–37.
17. Deutsch, T.F. Laser window materials—An overview. *J. Electron. Mater.* **1975**, *4*, 663–719. https://doi.org/10.1007/BF02661168.
18. Naumov, A.V.; Startsev, V.V. Germanium as a Photonics Substance: From Lenses to Dislocation-Free Wafers. *Photonics* **2023**, *17*, 114–132. https://doi.org/10.22184/1993-7296.FRos.2023.17.2.114.132.
19. Fortune Business Insights. Available online: https://www.fortunebusinessinsights.com/semiconductor-market-102365 (accessed on 28 January 2024).
20. Transparency Market Research. Available online: https://www.transparencymarketresearch.com/silicon-metal-market.html (accessed on 28 January 2024).
21. Kaplunov, I.A.; Kolesnikov, A.I. The effect of germanium features on IR scattering. *Poverkhnost Rentgenovskie Sinkhronnye i Nejtronnye Issledovaniya* **2002**, *2*, 14–20.
22. Kaplunov, I.A.; Smirnov, Y.M.; Kolesnikov, A.I. Optical transparency of crystalline germanium. *J. Opt. Technol.* **2005**, *72*, 214–220. https://doi.org/10.1364/JOT.72.000214.
23. Kaplunov, I.A.; Kolesnikov, A.I.; Shajovich, S.L.; Talyzin, I.V. Light scattering by single crystals of paratellurite and germanium. *J. Opt. Technol.* **2005**, *72*, 271–275. https://doi.org/10.1364/JOT.72.000271.
24. Kaplunov, I.A.; Kolesnikov, A.I.; Skokov, K.P.; Grechishkin, R.M.; Sedova, L.V.; Tret'yakov, S.A. The relationship between mechanical stresses and optical anomalies in germanium and paratellurite. *J. Opt. Technol.* **2005**, *72*, 572–576. https://doi.org/10.1364/JOT.72.000572.
25. Kaplunov, I.A.; Kolesnikov, A.I.; Shaiovich, S.L. Methods for Measuring Light Scattering in Germanium and Paratellurite Crystals. *Crystallogr. Rep.* **2005**, *50*, 546–552. https://doi.org/10.1134/1.2133971.
26. Kaplunov, I.A. How do the transmittances of crystals depend on their thickness? *J. Opt. Technol.* **2005**, *72*, 934–939. https://doi.org/10.1364/JOT.72.000934.
27. UOMZ. Available online: http://uomz.ru/ru/production/optical-observation-system/son-530 (accessed on 28 January 2024).
28. Tydex. Available online: http://www.tydexoptics.com/pdf/ru/ATR_Elements_ru.pdf (accessed on 28 January 2024).
29. Deymier, P.A. (Ed.) *Acoustic Metamaterials and Phononic Crystals*; Springer Series in Solid-State Sciences; Springer: Berlin/Heidelberg, Germany, 2013; Volume 173, 378p. https://doi.org/10.1007/978-3-642-31232-8.
30. Moss, T.S.; Barrel, G.J.; Ellis, B. *Semiconductor Opto-Electronics*; Butterworth-Heinemann: Oxford, UK, 2013; 454p.
31. Ross, M. *Laser Receivers; Devices, Techniques, Systems*; John Wiley: New York, NY, USA, 1966; 405p.
32. Kulchitsky, N.A.; Naumov, A.V.; Startsev, V.V. Infrared Focal Plane Array Detectors: "Post Pandemic" Development Trends. *Photonics* **2020**, *13*, 234–244. https://doi.org/10.22184/1993-7296.FRos.2020.14.3.234.244 234.
33. Darviot, Y.; Sorrentino, A.; Joly, B.; Pajot, B. Metallurgy and physical properties of mercury-doped germanium related to the performances of the infrared detector. *Infrared Phys.* **1967**, *7*, 1–10. https://doi.org/10.1016/0020-0891(67)90024-3.
34. Bratt, P.R. Impurity Germanium and Silicon Infrared Detectors. *Semicond. Semimet.* **1977**, *12*, 39–142. https://doi.org/10.1016/S0080-8784(08)60147-7.
35. Kimerling, L.C.; Wada, K. (Eds.) *Photonics and Electronics with Germanium*; Wiley: New York, NY, USA, 2015; 336p. ISBN 3527328211/9783527328215.
36. Shin, S.H.; Liao, Y.K.; Kim, M. A highly ordered and damage-free Ge inverted pyramid array structure for broadband antireflection in the mid-infrared. *J. Mater. Chem. C* **2021**, *9*, 9884–9891. https://doi.org/10.1039/d1tc01134k.
37. Grinberg, A.A. Theory of the Photoelectric and Photomagnetic Effects Produce by Light Pressure. *Sov. J. Exp. Theor. Phys.* **1970**, *31*, 531–534.
38. Agafonov, V.G.; Valov, P.M.; Ryvkin, B.S.; Yaroshetskii, I.D. Photodetectors based on the drag of carriers by photons in semiconductors. *Sov. Phys. Semicond.* **1974**, *7*, 1540–1545.
39. Gibson, A.F.; Kimmit, M.F.; Walker, A.C. Photon drag in Germanium. *Appl. Phys. Lett.* **1970**, *17*, 75–79. https://doi.org/10.1063/1.1653315.
40. Rogalin, V.E.; Filin, S.A.; Kaplunov, I.A. A Multirange Photodetector Based on the Effect of Photon Dragging Current Carriers in Germanium for High-Power Lasers in the Infrared Range. *Instrum. Exp. Tech.* **2019**, *62*, 679–682. https://doi.org/10.1134/S0020441219050087.
41. Artemyev, V.V.; Smirnov, A.D.; Kalaev, V.V.; Mamedov, V.M.; Sidko, A.P.; Podkopaev, O.I.; Kravtsova, E.D.; Shimansky, A.F. Modeling of dislocation dynamics in germanium czochralski growth. *J. Cryst. Growth* **2017**, *468*, 443–447. https://doi.org/10.1016/j.jcrysgro.2017.01.032.
42. Umicore. Available online: https://eom.umicore.com/en/germanium-solutions/products/high-purity-germanium-crystals (accessed on 31 August 2024).
43. Raut, M.-S.; Mei, H.; Mei, D.-M.; Bhattarai, S.; Wei, W.-Z.; Panth, R.; Acharya, P.; Wang, G.-J. Characterization of high-purity germanium (Ge) crystals for developing novel Ge detectors. *J. Instrum.* **2020**, *15*, T10010. https://doi.org/10.1088/1748-0221/15/10/T10010.
44. Abrosimov, N.; Czupalla, M.; Dropka, N.; Fischer, J.; Gybin, A.; Irmscher, K.; Janicskó-Csáthy, J.; Juda, U.; Kayser, S.; Miller, W.; et al. Technology development of high purity germanium crystals for radiation detectors. *J. Cryst. Growth* **2020**, *532*, 125396 https://doi.org/10.1016/j.jcrysgro.2019.125396.

45. Miller, W.; Sabanskis, A.; Gybin, A.; Gradwohl, K.-P.; Wintzer, A.; Dadzis, K.; Virbulis, J.; Sumathi, R. A Coupled Approach to Compute the Dislocation Density Development during Czochralski Growth and Its Application to the Growth of High-Purity Germanium (HPGe). *Crystals* **2023**, *13*, 1440. https://doi.org/10.3390/cryst13101440.
46. Sumathi, R.R.; Gybin, A.; Gradwohl, K.P.; Palleti, P.C.; Pietsch, M.; Irmscher, K.; Dropka, N.; Juda, U. Development of Large-Diameter and Very High Purity Ge Crystal Growth Technology for Devices. *Cryst. Res. Technol.* **2023**, *58*, 2200286. https://doi.org/10.1002/crat.202200286.
47. Ozhogin, V.I.; Inyushin, A.V.; Taldenko, A.N.; Tikhomirov, A.V.; Popov, G.E.; Haller, E.; Itoh, K. Isotope effect in the thermal conductivity of germanium single crystals. *JETP Lett*. **1996**, *63*, 490–494. https://doi.org/10.1134/1.567053.
48. Kaplunov, I.A.; Rogalin, V.E.; Gavalyan, M.Y. The Influence of Impurity and Isotopic Composition of Single-Crystal Germanium on Optical Transmission in the Range of 520–1000 cm^{-1}. *Optic. Spectrosc*. **2015**, *118*, 240–246. https://doi.org/10.1134/S0030400X15020083).
49. Kropotov, G.I.; Rogalin, V.E.; Kaplunov, I.A.; Shakhmin, A.A.; Filin, S.A.; Bulanov, A.D. Isotopic Shift in the IR of Germanium Single Crystals. *Opt. Spectrosc*. **2023**, *131*, 840–844. https://doi.org/10.61011/EOS.2023.06.56675.4334-22.
50. Fox, A. Acoustooptic Figure of Merit for Single Crystal Germanium at 10,6 μm Wavelength. *Appl. Opt*. **1985**, *24*, 2040–2041. https://doi.org/10.1364/AO.24.002040.
51. G&H Available online: https://goochandhousego.com (accessed on 19 February 2024).
52. Fox, A.J. Thermal design for germanium acoustooptic modulators. *Appl. Opt*. **1987**, *26*, 872–884. https://doi.org/10.1364/AO.26.000872.
53. Kanai, T.; Yoshihashi-Suzuki, S.; Ishii, K.; Awazu, K. Free electron laser pulse control by acousto-optic modulators. In Proceedings of the 27th International Free Electron Laser Conference, Stanford, CA, USA, 21–26 August 2005; BESSY: Berlin, Germany, 2006; pp. 427–430.
54. Fairley, P.D.; Rutt, H.N. Novel germanium infrared modulator. *J. Phys. D Appl. Phys*. **2000**, *33*, 2837–2852. https://doi.org/10.1088/0022-3727/33/21/325.
55. Shen, L.; Healy, N.; Mitchell, C.J.; Penades, J.S.; Nedeljkovic, M.; Mashanovich, G.Z.; Peacock, A.C. Mid-infrared all-optical modulation in low-loss germanium-on-silicon waveguides. *Opt. Lett*. **2015**, *40*, 268–271. https://doi.org/10.1364/OL.40.000268.
56. Soref, R.; Hendrickson, J.R.; Sweet, J. Simulation of germanium nanobeam electro-optical 2 × 2 switches and 1 × 1 modulators for the 2 to 5 μm infrared region. *Opt. Express* **2016**, *24*, 9369–9382. https://doi.org/10.1364/OE.24.009369.
57. Nesmelova, I.M.; Astaf 'ev, N.I.; Nesmelov, E.A. Resistivity dependence of the absorption coefficient of crystalline germanium in the IR region. *J. Opt. Technol*. **2007**, *74*, 71–74. https://doi.org/10.1364/JOT.74.000071.
58. Karlov, N.V.; Kirichenko, N.A.; Klimov, A.N.; Sisakyan, E.V. Investigation of the combined effects of CO2 and Nd laser radiation on germanium. *Sov. J. Quantum Electron*. **1983**, *13*, 887–891. https://doi.org/0.1070/QE1983v013n07ABEH004364.
59. Levinzon, D.I.; Rovinskij, R.E.; Rogalin, V.E.; Rykun, E.P.; Cenina, I.S.; Shershel', V.A. Pogloshchenie IK—Izlucheniya v germanii. In *Proc.Materialy IH sov. po polucheniyu profilirovannyh kristallov i izdelij sposobom Stepanova i ih primenenie v narodnom hozyajstve*; LIYaF: St. Petersburg, Russia, 1982; pp. 123–126. (In Russian)
60. Przhevuskiĭ, A.K.; Makolkina, E.N. The effect of plastic strain on the absorption spectrum of germanium crystals. *J. Opt. Technol.* **2007**, *74*, 135–138. https://doi.org/10.1364/jot.74.000135.
61. Kaplunov, I.A.; Kolesnikov, A.I. Low-angle boundaries in germanium. *Crystallogr. Rep*. **2004**, *49*, 184–187. https://doi.org/10.1134/1.1690412.
62. Shimanskii, A.F.; Podkopaev, O.I.; Molotkovskaya, N.O.; Kulakovskaya, T.V. Effect of the microstructure on electrical properties of high-purity germanium. *Phys. Solid State* **2013**, *55*, 949–951. https://doi.org/10.1134/S1063783413050296.
63. Rakwal, D.; Bamberg, E. Slicing, cleaning and kerf analysis of germanium wafers machined by wire electrical discharge machining. *J. Mater. Proc. Technol*. **2009**, *209*, 3740–3751. https://doi.org/10.1016/j.jmatprotec.2008.08.027.
64. Dimroth, F.; Kurtz, S. High efficiency multijunction solar cells. *MRS Bull*. **2007**, *32*, 230–235. https://doi.org/10.1557/mrs2007.27.
65. Shimanskii, A.F.; Kravtsova, E.D.; Kulakovskaya, T.V.; Grigorovich, A.P.; Kopytkova, S.A.; Smirnov, A.D. Investigation of the relationship between mechanical stresses, optical inhomogeneity, and the oxygen concentration in germanium crystals. *Semiconductors* **2022**, *56*, 2011–2206. https://doi.org/10.1134/S1063782622020129.
66. Shimanskii, A.F.; Gorodishcheva, A.N.; Pavluk, T.O.; Kopytkova, S.A. Effect of oxygen dissolved in germanium on defect formation and optical properties of single crystals. *IOP Conf. Ser. Mater. Sci. Eng*. **2019**, *467*, 012005. https://doi.org/10.1088/1757-899X/467/1/012005.
67. Talanin, V.I.; Talanin, I.E.; Matsko, O. Simulation of the creation of a defect structure of dislocation-free germanium single crystals. *J. Cryst. Growth* **2020**, *533*, 125472. https://doi.org/10.1016/j.jcrysgro.2019.125472.
68. Ryabov, A.I.; Spitsyn, V.I.; Stel'makh, N.S.; Pirogova, G.N. Effect of Radiation on the Optical Properties of High-Resistivity Ge, GaAs, and ZnSe Single Crystals. *Izv. Akad. Nauk SSSR Neorg. Mater*. **1977**, *13*, 27–30.
69. Litvinov, V.V.; Petukh, A.N.; Pokotilo, J.M.; Markevich, V.P.; Lastovskii, S.B. Formation and annealing of radiation defects in tin-doped p-type germanium crystals. *Semiconductors* **2012**, *46*, 611–614. https://doi.org/10.1134/S1063782612050156.
70. Fukuoka, N.; Yamaji, H.; Honda, M.; Atobe, K. Radiation defects in germanium. radiation defects annealed at ~260 °C in n-type germanium. *Radiat. Eff. Defects Solids* **1992**, *124*, 429–435. https://doi.org/10.1080/10420159208228869.
71. Peplowski, P.N.; Burks, M.; Goldsten, J.O.; Fix, S.; Heffern, L.E.; Lawrence, D.J.; Yokley, Z.W. Yokley Radiation damage and annealing of three coaxial n-type germanium detectors: Preparation for spaceflight missions to asteroid 16 Psyche and Mars'

moon Phobos. *Nucl. Instrum. Methods Phys. Res. Sect. A Accel. Spectrometers Detect. Assoc. Equip.* **2019**, *942*, 162409. https://doi.org/10.1016/j.nima.2019.162409.
72. Brown, W.L.; Augustyniak, W.M.; Waite, T.R. Annealing of Radiation Defects in Semiconductors. *J. Appl. Phys*. **1959**, *30*, 1258–1268. https://doi.org/10.1063/1.1735303.
73. Algora, C.; García, I.; Delgado, M.; Peña, R.; Vázquez, C.; Hinojosa, M.; Rey-Stolle, I. Beaming power: Photovoltaic laser power converters for power-by-light. *Joule* **2020**, *6*, 340–368. https://doi.org/10.1016/j.joule.2021.11.014.
74. Allwood, G.A.; Wild, G.; Hinckley, S. A Comparison of InGaAs and Ge photonic power converters for long wavelength power over fibre. In Proceedings of the COMMAD 2012, Melbourne, VIC, Australia, 12–14 December 2012. https://doi.org/10.1109/COMMAD.2012.6472337.
75. Allwood, G.; Wild, G.; Hinckley, S. A Comparison of Silicon and Germanium Photovoltaic Power Conversion for Power-Over-Fibre. *Smart Nano-Micro Mater. Devices* **2011**, *820410*, 152–162. https://doi.org/10.1117/12.903294.
76. Hvostikova, O.A.; Sorokina, S.V.; Shvarc, M.Z.; Ber, B.Y.; Kazancev, D.Y.; Hvostikov, V.P. Fotoelektricheskij priemnik lazernogo izlucheniya na osnove germaniya. *ZHTF* **2024**, *94*, 801–807. https://doi.org/10.61011/JTF.2024.05.57819.297-23. (In Russian)
77. Zhernov, A.P.; Inyushkin, A.V. Kinetic coefficients in isotopically disordered crystals. *Phys.–Usp*. **2002**, *45*, 527–552 https://doi.org/10.1070/PU2002v045n05ABEH001084.
78. Kuleev, I.G.; Kuleev, I.I. Anisotropic attenuation of transverse ultrasound in cubic crystals of Ge, Si, and diamond with various isotopic compositions. *Phys. Solid State* **2007**, *49*, 1643–1651. https://doi.org/10.1134/S1063783407090077.
79. Apollonov, V.V.; Vas′kovskiĭ, Y.M.; Zhavoronkov, M.I.; Prokhorov, A.M.; Rovinskiĭ, R.E.; Rogalin, V.E.; Ustinov, N.D.; Firsov, K.N.; Tsenina, I.S.; Yamshchikov, V.A. High-power electric-discharge CO_2 laser with easily ionizable substances added to the mixture. *Sov. J. Quantum Electron*. **1985**, *15*, 1–3. https://doi.org/10.1070/QE1985v015n01ABEH005831.
80. Rogalin, V.E. Effect of Absorbing Microinhomogeneities on Optical Damage to Alkali–Halide Crystals. *Bull. Russ. Acad. Sci. Phys*. **2012**, *76*, 1205–1216. https://doi.org/10.3103/S1062873812110184.
81. Mikolutskiy, S.I.; Khasaya, R.R.; Khomich, Yu.V.; Yamshchikov, V.A. Formation of various types of nanostructures on germanium surface by nanosecond laser pulses. *J. Phys. Conf. Ser*. **2018**, *987*, 012007. https://doi.org/10.1088/1742-6596/987/1/012007
82. Levinzon, D.I.; Rovinskij, R.E.; Rogalin, V.E.; Rykun, E.P.; Trajnin, A.L.; Tsenina, I.S.; Shejhet, E.G. Issledovanie monokristallov profil′nogo germaniya, obluchyonnyh impul′snym CO_2—Lazerom. *Izv. AN USSR. Ser. fiz*. **1979**, *43*, 2001–2005. (In Russian)
83. Noller, B.M.; Drescher, B.; Gillot, C.; Li, Y. A Method for the Manufacture of Semiconductor Devices Involving the Chemical-Mechanical Polishing of Elemental Germanium and/or $Si_{1-x}Ge_x$ Material in the Presence of a CMP (Chemical-Mechanical Polishing) Composition Comprising a Special Organic Compound. Patent RU 2605941, 30 July 2012.
84. Zubov, B.V.; Manenkov, A.A.; Milyaev, V.A.; Mikhailova, G.N.; Murina, T.M.; Seferov, A.S. Microwave absorption by nonequilibrium carriers in germanium. Method for determination of carrier density. *Sov. Phys. Solid State* **1976**, *18*, 406–410.
85. Seo, D.; Gregory, J.M.; Feldman, L.C.; Tolk, N.H.; Cohen, P.I. Multiphoton absorption in germanium using pulsed infrared free-electron laser radiation. *Phys. Rev. B* **2011**, *83*, 195203. https://doi.org/10.1103/PhysRevB.83.195203.
86. Alekseev, E.E.; Firsov, K.N.; Kazantsev, S.Y.; Kononov, I.G.; Rogalin, V.E. Nonlinear Absorption of Non-Chain HF Laser Radiation in Germanium. *Phys. Wave Phenom*. **2017**, *25*, 280–288. https://doi.org/10.3103/S1541308X17040070.
87. Basov, N.G.; Zel′dovich, B.Y.; Kovalev, V.I.; Faĭzullov, F.S.; Fedorov, V.B. Reflection of a multifrequency signal in four-wave interaction in germanium at 10.6 μm. *Sov. J. Quantum Electron*. **1981**, *11*, 514. https://doi.org/10.1070/QE1981v011n04ABEH006871.
88. Hall, J.L. Nobel Lecture: Defining and measuring optical frequencies. *Rev. Modern Phys*. **2006**, *78*, 1279–1295. https://doi.org/10.1103/RevModPhys.78.1279.
89. Kippenberg, T.J.; Gaeta, A.L.; Lipson, M.L.; Gorodetsky, M.L. Dissipative Kerr solitons in optical microresonators. *Science* **2018**, *361*, eaan8083. https://doi.org/10.1126/science.aan8083.
90. Riemensberger, J.; Lukashchuk, A.; Karpov, M.; Weng, W.; Lucas, E.; Liu, J.; Kippenberg, T.J. Massively parallel coherent laser ranging using a soliton microcomb. *Nature* **2020**, *581*, 164–170. https://doi.org/10.1038/s41586-020-2239-3.
91. Marin-Palomo, P.; Kemal, J.; Karpov, M.; Kordts, A.; Pfeifle, J.; Pfeiffer, M.H.P.; Trocha, P.; Wolf, S.; Brasch, V.; Anderson, M.H.; et al. Microresonator-based solitons for massively parallel coherent optical communications. *Nature* **2017**, *546*, 274–279. https://doi.org/10.1038/nature22387.
92. Tebeneva, T.S.; Lobanov, V.E.; Chermoshentsev, D.A.; Min′kov, K.N.; Kaplunov, I.A.; Vinogradov, I.I.; Bilenko, I.A.; Shitikov, A.E. Crystalline germanium high-Q microresonators for mid-IR. *Opt. Express* **2024**, *32*, 15680–15690. https://doi.org/10.1364/OE.521499.
93. Witteman, W.J. *The CO_2 Laser*; Springer: Berlin/Heidelberg, Germany, 1987; 309p.
94. Magdich, L.N.; Molchanov, V.Y. *Acoustooptic Devices and Their Applications*; Gordon and Breach Science Publishers: New York, NY, USA, 1989; 160p.
95. Korpel, A. *Acousto-Optics, Second Edition, Optical Science and Engineering*; CRC Press: Boca Raton, FL, USA, 1996; 360p. ISBN-13 978-0824797713.
96. Vinokurov, N.A.; Shevchenko, O.A. Free electron lasers and their development at the Budker Institute of Nuclear Physics, SB RAS. *Phys.-Usp*. **2018**, *61*, 435. https://doi.org/10.3367/UFNe.2018.02.038311.
97. Tydex. Available online: https://www.tydexoptics.com/ru/materials/materials_for_nonlinear_optics/germanium/ (accessed on 19 February 2024).

98. Kazantsev, S.Y.; Brusentsev, A.S.; Titovets, P.A.; Bellune, K.M.; Bogachev, N.N. Configurable plasma antenna with laser control. In Proceedings of the 2022 Systems of Signals Generating and Processing in the Field of on Board Communications, Moscow, Russia, 15–17 March 2022. https://doi.org/10.1109/IEEECONF53456.2022.9744361.
99. Bogachev, N.N.; Gusein-zadea, N.G.; Zhluktova, I.V.; Kazantsev, S.Y.; Kamynin, V.A.; Podlesnykh, S.V.; Rogalin, V.E.; Trikshev, A.I.; Filatova, S.A.; Tsvetkov, V.B.; et al. Semiconductor Plasma Antennas Formed by Laser Radiation. *Tech. Phys. Lett.* **2019**, *45*, 1223–1225. https://doi.org/10.1134/S1063785019120174.
100. Haight, R.; Ross, F.M.; Hannon, J.B. (Eds.) *Handbook of Instrumentation and Techniques for Semiconductor Nanostructure Characterization*; World Scientific Publishing Co Pte Ltd.: Singapore, 2011; 2 Volumes, 680p. https://doi.org/10.1142/7898.
101. Zheleznov, V.Y.; Malinskii, T.V.; Rogalin, V.E.; Khomich, Y.V.; Yamshchikov, V.A.; Kaplunov, I.A.; Ivanova, A.I. Effect of Nanosecond Ultraviolet Laser Pulses on the Surface of Germanium Single Crystals. *Russ. Microelectron*. **2023**, *52*, 741–749. https://doi.org/10.1134/S1063739723080073.
102. Zheleznov, V.Y.; Malinskiy, T.V.; Mikolutskiy, S.I.; Rogalin, V.E.; Filin, S.A.; Khomich, Y.V.; Yamshchikov, V.A.; Kaplunov, I.A.; Ivanova, A.I. Laser Etching of Germanium. *Tech. Phys. Lett*. **2021**, *47*, 705–707. https://doi.org/10.1134/S1063785021070282.
103. Blaker, J. Warren; Schaeffer, Peter. *Optics: An Introduction for Technicians and Technologists*; Prentice Hall: Hoboken, NJ, USA, 1999; 229p. ISBN 978-0132277945.
104. Weber, M.J. *Handbook of Lasers*; CRC Press: Boca Raton, FL, USA, 2001; 1198p.
105. Voloshinov, V.B.; Nikitin, P.A.; Gerasimov, V.V.; Knyazev, B.A.; Choporova, Y.Y. Deflection of a monochromatic THz beam by acousto-optic methods. *Quantum Electron*. **2013**, *43*, 1139–1142. https://doi.org/10.1070/QE2013v043n12ABEH015195.
106. Kropotov, G.I.; Kaplunov, I.A.; Rogalin, V.E.; Shakhmin, A.A.; Bulanov, A.D. Particular of radiation transmission of monoisotopic germanium single crystals in the terahertz spectral range. *Appl. Phys*. **2024**, *24*, 80–84. https://doi.org/10.51368/1996-0948-2024-1-63-67. (In Russian)